A Vibration Technique for Promoting Liquid Mixing and Reaction in a Microchannel

Yasumasa Ito and Satoru Komori
Dept. of Mechanical Engineering and Science, and Advanced Research Institute of Fluid Science and Engineering, Kyoto University, Kyoto 606-8501, Japan

DOI 10.1002/aic.10919
Published online June 16, 2006 in Wiley InterScience (www.interscience.wiley.com).

A vibration technique for promoting fluid mixing and chemical reaction in a microchannel was proposed, and the effects of the mechanical vibration on mixing and reaction were experimentally examined. The fluids before flowing into a microchannel were oscillated by a small vibrating motor through two tubes connected to the channel. Instantaneous velocity and concentration were measured using micro PIV and LIF techniques, respectively. The results show that fluid mixing and chemical reaction is remarkably promoted by the proposed vibration technique. The mixing rate is well correlated with the maximum rms value of normalized fluid velocity fluctuation in a microchannel. When the basic frequency of the mechanical vibration is low, the fluid motion hardly changes and the mixing and reaction is little enhanced. However, with increasing the frequency, almost complete mixing and reaction can be accomplished at the high frequency more than 90Hz by the proposed technique. © 2006 American Institute of Chemical Engineers *AIChE J,* 52: 3011–3017, 2006
Keywords: mixing enhancement, chemical reaction, vibration, microfluidics, microreactor

Introduction

Microfabrication techniques have recently developed a variety of micro devices, such as micro reactors, micro chemical plants, and microTAS.[1,2] These devices are employed in chemical, medical, and biological analysis to reduce analyzing time and sampling volumes. The productivity by using a great number of micro devices through replication may exceed that of the conventional macroscopic systems. It is, therefore, of great importance to investigate the details of the reactive-diffusive mechanism in a microchannel flow and to propose a method for promoting fluid mixing and chemical reaction in a microchannel.

Reactive fluids are usually introduced into a chemical reactor under non-premixed conditions. Accordingly, it is necessary to deform the interface of reactive fluids complicatedly for promoting rapid mixing and reaction,[3,4] since the chemical reaction proceeds through the molecules diffusion at the interface between the two reactive fluids. The flow in a macroscopic reactor is usually turbulent and the interface can easily be deformed. On the other hand, the flow in a microchannel is predominantly laminar and it is considered to be difficult to rapidly mix the fluids. Consequently, most of the previous research on the enhancement of mixing and reaction in a microchannel has been focused on the passive methods: increasing the channel length and crossing the channels in order to gain the long time needed for molecular diffusion of reactants.[5-10] Moreover, chaotic advection due to the complex configuration of channels has been used to promote fluid mixing.[9,11] However, a microchannel is so thin that the large pressure drop due to the complicated and lengthened channel often causes serious problems. Besides, as the driving force of fluid mixing in such devices is only molecular diffusion, it requires a long time to accomplish sufficient mixing.

For the above reasons, it is required to develop a technique based on the use of additional force for promoting fluid mixing in a simple microchannel, as well as in macroscopic reactors. Some techniques utilizing time pulsing,[12] ultrasound,[13] electrokinetic effects,[14,15] and magnetohydrodynamic (MHD) effects[16] have been proposed for such purposes, but their appli-

Correspondence concerning this article should be addressed to S. Komori at komori@mech.kyoto-u.ac.jp.

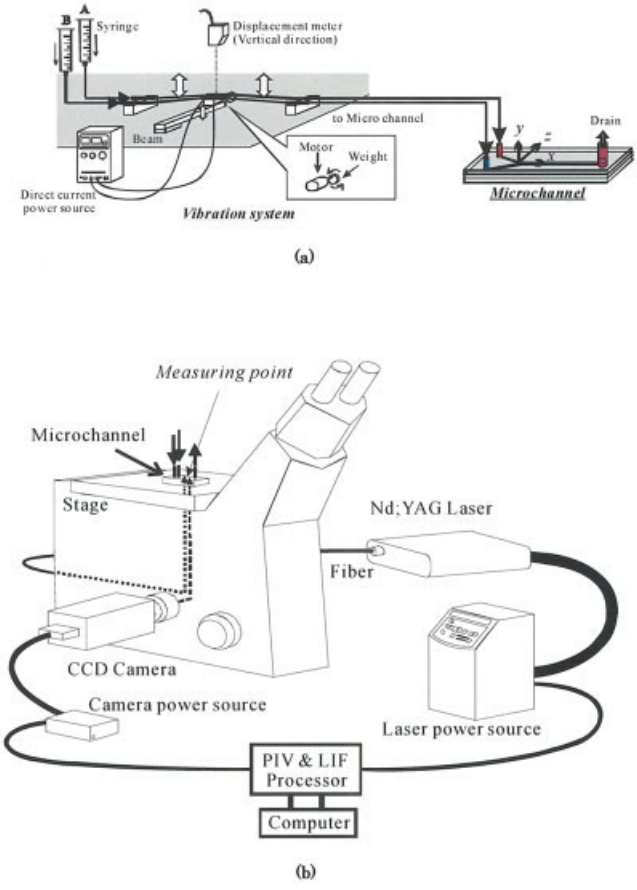

Figure 1. Experimental setup.

(a) The vibration system and microchannel; (b) Measuring system. [Color figure can be viewed in the online issue, which is available at www.interscience.wiley.com.]

cations have been limited. Obviously, it is not practical to install an active object such as a stirrer in a microchannel.

From these points of view, we proposed a simple vibration technique[17] based on the usage of a small vibrating motor as an innovative method for promoting fluid mixing and chemical reaction in a microchannel without directly contacting fluids. The purpose of this article is to introduce an original technique and to examine the effects of the technique on mixing and reaction by carrying out comprehensive experiments.

Experimental

Figure 1 shows: (a) the Y-shaped microchannel and the vibration system, and (b) the measuring system. The channel was constructed by holding a thin stainless plate (channel layer) between two transparent polymethylemethacrylate (PMMA) plates (top- and bottom-wall layers). A Y-shaped groove was cut as a single channel in the channel layer of the stainless plate, and two holes for inlets and a hole for an outlet were drilled out in the top-wall layer of the PMMA plate. The three layers were sandwiched. Two fluids were separately supplied from syringes to the channel by a syringe pump (Harvard PHD2000) through two polyethylene introductory tubes with the diameter of 1mm. The vibration system was constructed by a beam (10 mm in width, 2 mm in height, and 90 mm in length) and a small vibrating motor with an eccentric weight. As the motor was attached on the tip of the beam, the tubes contacted on the beam were monolithically vibrated together with the beam and motor by the rotation of the eccentric weight. The tubes were fixed at a distance of 100mm from the vibrating point on the beam in both the upstream and downstream directions so that only the 200mm part of the tube between the fixed points was mechanically vibrated. The electrical input for the motor, V_{in}, was supplied by a DC-stabilizing power supply (KENWOOD PA18–2A), and it was changed in the range of 0 ~ 2.0V to control the vibration frequency.

Table 1. Experimental Conditions

Run	I [mm]	Q [ml/min]	$\bar{U}_a$ [m/s]	Re
Run I	0.5	0.2	0.0133	6.7
Run II	0.5	2.0	0.133	67
Run III	0.1	0.008	0.0133	1.3
Run IV	0.1	0.04	0.0667	6.7
Run V	0.1	0.2	0.333	33

The experimental conditions are listed in Table 1. The cross-sectional area of the channel used in Runs I and II was 0.5×0.5 mm^2. Both species A and species B were supplied at the flow rate of $Q_A = Q_B = 0.1$ml/min in Run I. The flow rate in Run II was set to 10 times larger than that in Run I. On the other hand, the channel used in Runs III ~ V had the cross-sectional area of 0.1×0.1 mm^2. The cross-sectional mean velocity, $\bar{U}_a$, in Run III, the Reynolds number based on the mean velocity and the channel width, Re, in Run IV, and the total flow rate, $Q(=Q_A + Q_B)$, in Run V, were set to the same values as those in Run I, respectively. The channel length was 60 mm in all cases. Experiments with different flow rate ratios (Q_A/Q_B = 1, 1/2, 1/5, and 1/10) were additionally carried out under the conditions of Run I.

Instantaneous fluid velocity and concentration were measured using the micro PIV (Particle Image Velocimetry) and LIF (Laser Induced Fluorescence) techniques (Dantec 80N system), respectively, as shown in Figure 1b. The Nd:YAG laser (wave length: λ = 532 nm; New Wave Research Solo PIV III-15) was introduced from the bottom of the channel to the measuring point. The spatial resolution of the digital CCD camera (Hi Sence) was 1280 × 1024 pixels for the imaging area of 0.868×0.695 mm^2 (Runs I and II) or 0.135×0.109 mm^2 (Runs III ~ V). Table 2 lists chemical components used for non-reacting and reacting flows. For the concentration measurement in a non-reacting flow, Rhodamine B ($C_{28}H_{31}N_2O_3Cl$) solution with the concentration of 8.7×10^{-6} mol/l for Runs I and II and 7.0×10^{-5} mol/l for Runs III ~ V and distilled water were used as non-reacting species A and B, respectively. In order to visualize the chemical product in a reacting flow, Rhod-2 ($C_{40}H_{43}ClN_4O_{11}$) solution with the concentration of 5.0×10^{-6} mol/l and calcium chloride($CaCl_2$) solution with the concentration of 1.0×10^{-4} mol/l were used as reactive species A and B, respectively. Rhod-2 is a fluorescein that has a Rhodamine moiety, and it fluoresces by chelat-

Table 2. Combinations of Species A and B

Flow Type	Species A	Species B
Non-reacting	Rhodamine B	H_2O
Reacting	Rhod-2	$CaCl_2$

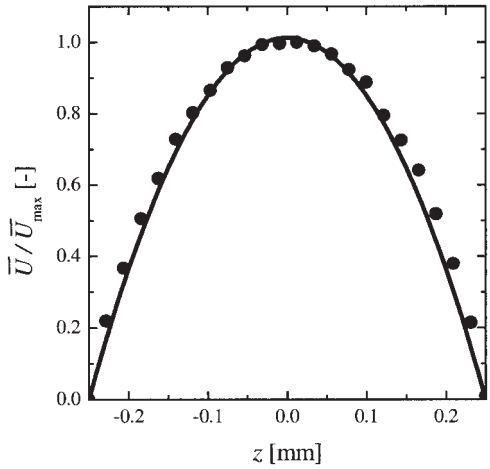

Figure 2. Spanwise distribution of the mean streamwise fluid velocity in a microchannel (Run I).

A solid line shows the Poiseuille flow distribution.

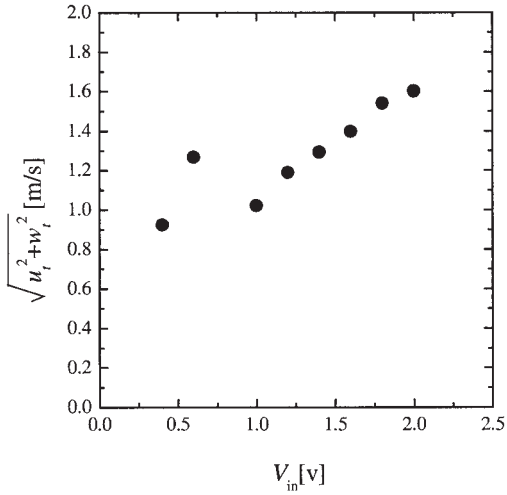

Figure 3. Relationship between the electrical input for a vibrating motor and the rms value of vibrating tube-velocity fluctuation.

ing with Ca^{2+} ion. Hence, the produced complex ion ($[C_{40}H_{39}CaN_4O_{11}]^-$) can be visualized as a chemical product by the LIF. The reaction rate constant between Rhod-2 and $CaCl_2$ was the order of 10^6 m^3 mol^{-1} s^{-1}, and the reaction can be regarded as a rapid reaction. Note that a tiny amount of EGTA ($C_{14}H_{24}N_2O_{10}$) was pre-mixed in species A to completely eliminate Ca^{2+} ion, which initially exists in the solution. For the velocity measurements, tracer particles (Duke Science Corp. R900) were dispersed in both the fluids. The measurements were conducted around 8mm downstream of the flow junction (the root of the Y-shaped channel) and at the center of the channel in the vertical direction. The sampling frequency for fluid velocity and concentration signals was 2Hz, and 100 images were processed to calculate statistics by the PIV and LIF data processor (DANTEC Flow Manager). In the supplementary experiment for making the calibration curve between the digitalized fluorescence intensity and the concentration of species A, the normalized standard deviation of the digitalized fluorescence intensity for a concentration of species A was 8.3%. Therefore, the potential error of the concentration was estimated to be 8.3%.

The displacements of the introductory beam in the vertical and streamwise directions were measured by the laser displacement meter (KEYENCE LB-02). Since the two introductory tubes were fixed on the beam, the tube displacement was equivalent to that of the beam. The displacement measurement was carried out at the sampling frequency of 3kHz for 20 s. The coordinates of x, y, and z denote the streamwise, vertical, and spanwise directions, respectively.

Results and Discussion

Relationship between tube-vibration fluctuation and fluid velocity fluctuation

Figure 2 shows the spanwise distribution of the mean velocity, $\bar{U}$, in the non-vibrating flow of Run I, together with the distribution of the Poiseuille flow. Here, $\bar{U}$ is normalized by the maximum mean velocity, $\bar{U}_{max}$. The good agreement between the measured $\bar{U}$ and the Poiseuille flow distribution indicates that a typical laminar flow is formed in the microchannel.

Figure 3 shows the relationship between the electrical input for a vibrating motor, V_{in}, and the rms value of vibrating tube-velocity fluctuation, $\sqrt{u_t^2 + w_t^2}$ in Run I. The tube-velocity fluctuation increases with the electrical input in the region of $V_{in} \geq 1.0$V, but $\sqrt{u_t^2 + w_t^2}$ around $V_{in} = 0.6$V is larger than those for $1.0\text{V} \leq V_{in} \leq 1.4\text{V}$. In order to explain this large value, the basic vibration frequency, f_b, was determined by computing the power spectrum of the vertical tube-velocity fluctuation, as shown in Figure 4. The power spectrum, S_v, is defined by

$$\overline{v^2} = \int_0^\infty S_v(f)d(f). \tag{1}$$

It is found that the vibration amplitude in the vertical direction, A_t, and the basic frequency, f_b, for $V_{in} = 0.4$V and 0.6V are about $f_b = 17 \sim 21$Hz and $A_t = 20 \sim 28$mm, respectively,

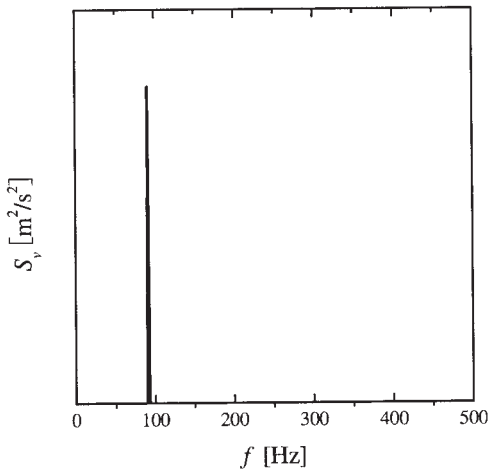

Figure 4. An example of the power spectrum of the vertical vibrating tube-velocity fluctuation.

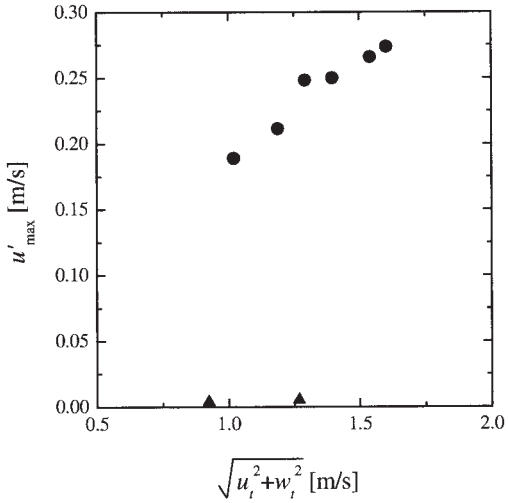

Figure 5. Relationship between the maximum rms value of streamwise fluid velocity fluctuation and the rms value of vibrating tube-velocity fluctuation in Run I.

(●) f_b = 17 ~ 21Hz; (▲) f_b = 75 ~ 92Hz.

whereas those for V_{in} = 1.0 ~ 2.0V were f_b = 75 ~ 92Hz and A_t = 3.9 ~ 4.2mm, respectively. In other words, the tube (beam) slowly vibrates with large amplitude for V_{in} = 0.4V and V_{in} = 0.6V, whereas it quickly vibrates with small amplitude for V_{in} = 1.0 ~ 2.0V.

Figure 5 shows the relationship between the maximum rms value of streamwise fluid velocity fluctuation, u'_{max} ($=\sqrt{u^2_{max}}$), and the rms value of vibrating tube-velocity fluctuation, $\sqrt{u_t^2 + w_t^2}$. The u'_{max} was observed in the central region of the channel, as shown in Figure 6. The data in Figure 5 can be divided into two groups as shown by two symbols. The triangle (▲) and circle (●) show the data for the basic frequency of mechanical vibration, f_b, of 17 ~ 21Hz and the data for f_b = 75 ~ 92Hz, respectively. For f_b = 75 ~ 92Hz, u'_{max} is almost proportional to $\sqrt{u_t^2 + w_t^2}$, whereas u'_{max} for f_b = 17 ~ 21Hz

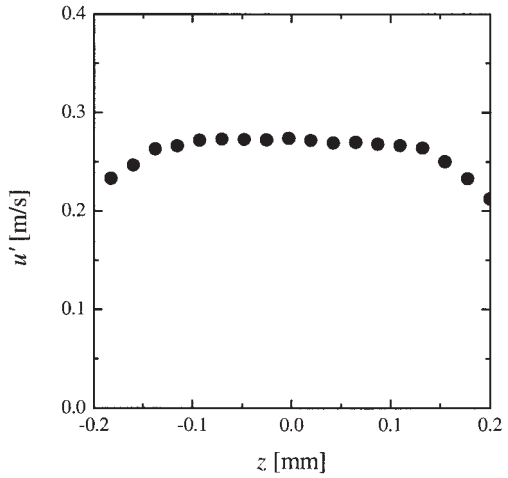

Figure 6. Spanwise distribution of the rms value of streamwise fluid velocity fluctuation in Run I (V_{in} = 2.0V).

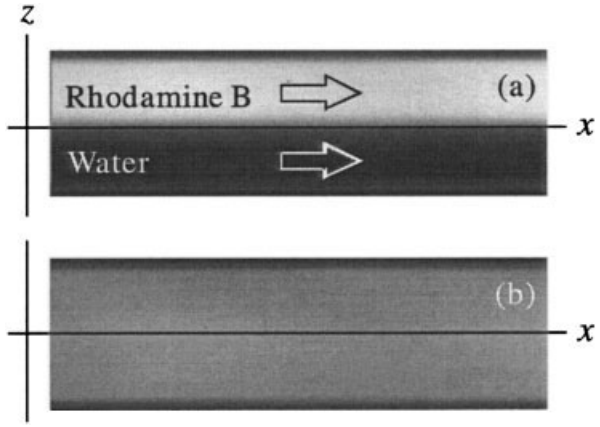

Figure 7. Snapshots of mixing conditions around x = 8 mm in a microchannel.

(a) No vibration (V_{in} = 0V); (b) Strong vibration with f_b = 92Hz (V_{in} = 2.0V).

does not increase with increasing u'_{max}. In the case of f_b = 17 ~ 21Hz, the vibration is slow and the interface of the fluids is little deformed. On the contrary, in the cases of f_b = 75 ~ 92Hz, the tubes quickly vibrate and the fluids are intensely disturbed in the channel. The differences in mixing conditions are discussed in the next paragraph.

Mixing rate

Figure 7 shows the snapshots of mixing conditions around x = 8mm in: (a) non-vibrating (f_b = 0Hz) and (b) vibrating (f_b = 92Hz) flows in Run I. It is found that the two fluids in a non-vibrating flow are almost completely separated, although fluid mixing is slightly progressed at the center of the channel through molecular diffusion. On the other hand, fluid mixing is remarkably promoted in the vibrating flow and almost complete mixing is accomplished.

To quantitatively estimate the mixing condition, the normalized concentration of species A, C_A, was digitized by the LIF, and the mixing rate, $\bar{\phi}$, was calculated. Figure 8 shows the spanwise distributions of the concentration of species A, C_A, at x = 8mm under the same conditions as in Figure 7. The symbols of triangle (▲) and circle (●) correspond to the cases of: (a) non-vibrating and (b) vibrating conditions as in Figures 7(a) and (b), respectively. When the flow rate ratio of two fluids, Q_A/Q_B, is equal to $1/\alpha$, the concentration of species A at the complete mixing, C_1, is expressed as

$$C_1 = \frac{1}{1+\alpha} \tag{2}$$

Then, the instantaneous local mixing rate at each interrogation area, ξ, is defined as

$$\xi = \frac{C_A}{C_1}, \qquad (C_A \le C_1)$$

$$\xi = \frac{1-C_A}{1-C_1}. \qquad (C_A \ge C_1) \tag{3}$$

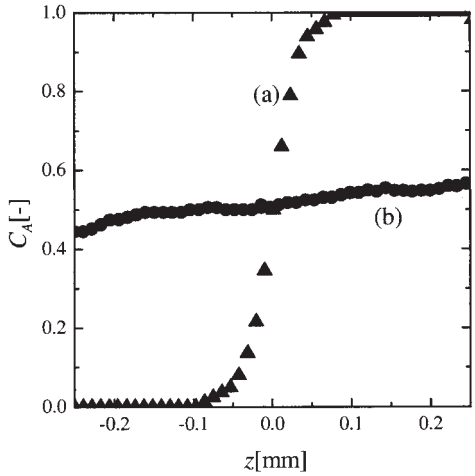

Figure 8. Spanwise distributions of the normalized concentration of species A, C_A.

(▲) No vibration (V_{in} = 0V); (●) Strong vibration with f_b = 92Hz (V_{in} = 2.0V).

This definition of ξ indicates that the two chemical species are homogeneously mixed when the complete mixing is accomplished. That is, the normalized concentrations of completely mixed non-reacting species A and B must be $1/(1 + \alpha)$ and $\alpha/(1 + \alpha)$ at all points on the cross-section of the microchannel, respectively.

The relation between ξ and C_A is also shown in Figure 9. The instantaneous mixing rate at the cross section, ϕ, is calculated by averaging ξ in the spanwise (z) direction. When ϕ at the k-th image is expressed by ϕ_k, the mixing rate, $\bar{\phi}$, is finally obtained by ensemble-averaging ϕ:

$$\phi = \frac{1}{l}\int_{-l/2}^{l/2} \xi dz \tag{4}$$

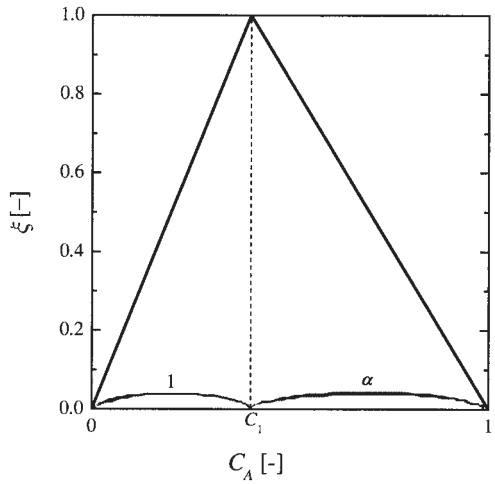

Figure 9. Relationship between the local mixing rate and concentration of species A.

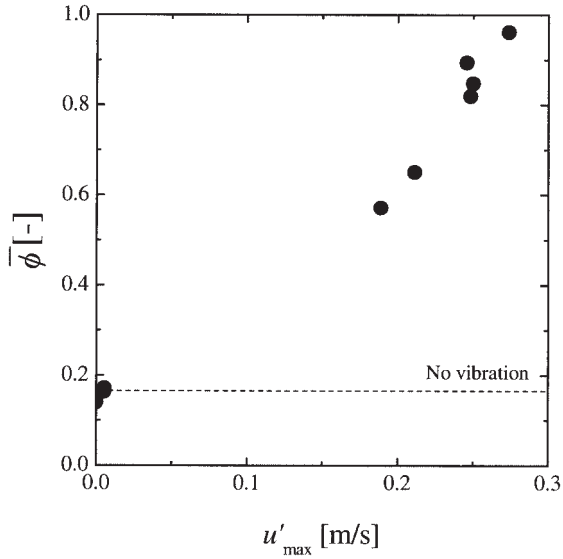

Figure 10. Relationship between the mixing rate and the maximum rms value of streamwise fluid velocity fluctuation in Run I.

$$\bar{\phi} = \frac{1}{n}\sum_{k=1}^{n} \phi_k \tag{5}$$

where l is the channel width and n is the number of the images used for averaging.

Relationship between fluid fluctuation and mixing rate

Figure 10 shows the relationship between the mixing rate, ϕ, and the maximum rms value of streamwise fluid velocity fluctuation, u'_{max}, in Run I. It is found that the mixing rate is well correlated with the intensity of fluid velocity fluctuation. This result, together with the result in Figure 5, also suggests that the mixing rate is not correlated with the intensity of the tube-velocity fluctuation.

To examine the applicability of the proposed vibration technique for different flow rate ratio cases, experiments for four flow rate ratios of Q_A/Q_B = 1, 1/2, 1/5, and 1/10 were conducted under the conditions of Run I. The mixing rates, ϕ, against u'_{max} are shown in Figure 11. It is proved that the proposed vibration technique is useful for promoting fluid mixing, regardless of the flow rate ratio.

Figure 12 shows the relationship between the mixing rate, ϕ, and normalized maximum rms value of streamwise fluid velocity fluctuation, u'_{max}, by the mean velocity, $\bar{U}_a$, for Runs I-V in the two channels with different cross-sectional area. The relationships show that the mixing rate is well correlated with the normalized maximum rms value of streamwise velocity fluctuation, $u'_{max}/\bar{U}_a$, and the proposed vibration technique is an efficient method for promoting fluid mixing in both channels with the cross-sectional area of 0.1 × 0.1 mm^2 and 0.5 × 0.5 mm^2. It is found that the mixing is hardly promoted at all when the flow rate is large. This is because the fluid velocity is too fast and the time scale for mixing is too short. Furthermore, these results suggest that stronger vibration is required for

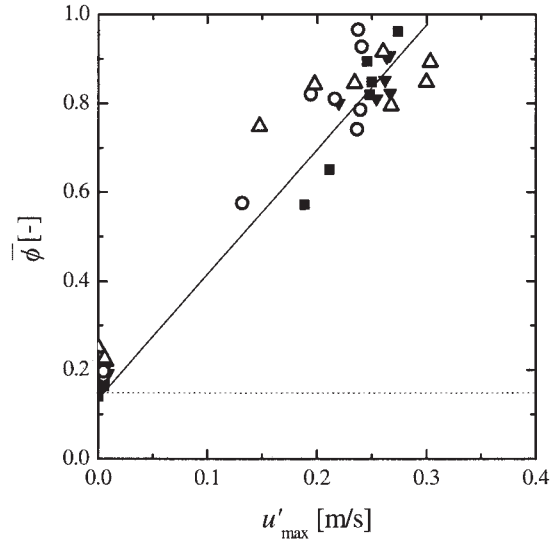

Figure 11. Relationship between the mixing rate and the maximum rms value of streamwise fluid velocity fluctuation in the cases with different flow rate ratios of Q_A/Q_B in Run I.

(■) Q_A/Q_B = 1; (▼) Q_A/Q_B = 1/2; (○) Q_A/Q_B = 1/5; (△) Q_A/Q_B = 1/10.

promoting fluid mixing for large flow rate, and the magnitude of the streamwise fluid velocity fluctuation should be more than 10 times as large as the mean velocity to accomplish complete mixing.

The remarkable enhancement of the mixing and reaction by the proposed technique mainly occurs at the flow junction and it may be attributed to the pressure fluctuation generated in the channel by the mechanical vibration. However, we couldn't directly verify it, since it was difficult to measure the pressure in the microchannel.

In order to observe the reacting conditions, chemical product in Run I is visualized by the LIF, as shown in Figure 13. The chemical product is produced only in the central region of the microchannel in the non-vibrating flow (Figure 13(a)). In contrast, the chemical product is produced in all the region of the channel in the vibrating flow (Figure 13(b)). These results support that the chemical reaction is promoted by the proposed vibration technique. However, quantitative evaluation of the chemical product couldn't be conducted, since it was impossible to obtain a reliable calibration curve between the fluorescence intensity and the concentration of the chemical product.

Conclusions

A simple vibration technique using a small vibrating motor was proposed as a new technique for promoting fluid mixing and chemical reaction in a microchannel, and the promotion efficiency was experimentally investigated. The results are summarized as follows: Fluid mixing and chemical reaction is remarkably enhanced by the proposed vibration technique.

The mixing rate is well correlated with the maximum rms value of streamwise fluid velocity fluctuation normalized by the mean velocity. Fluid velocity fluctuation more than 10 times larger than the mean velocity is required for accomplishing the complete mixing.

When the basic vibration frequency is low, the amplitude of the tube vibration is large, but the vibration is slow. Therefore, the interface of the fluids in a microchannel is little deformed. On the contrary, when the basic vibration frequency is high, the tubes quickly vibrate and the fluids in the tubes fluctuate remarkably. This results in strong promotion of fluid mixing and reaction.

Our additional experiments proved that the same promotion performance for mixing and reaction can be obtained even in

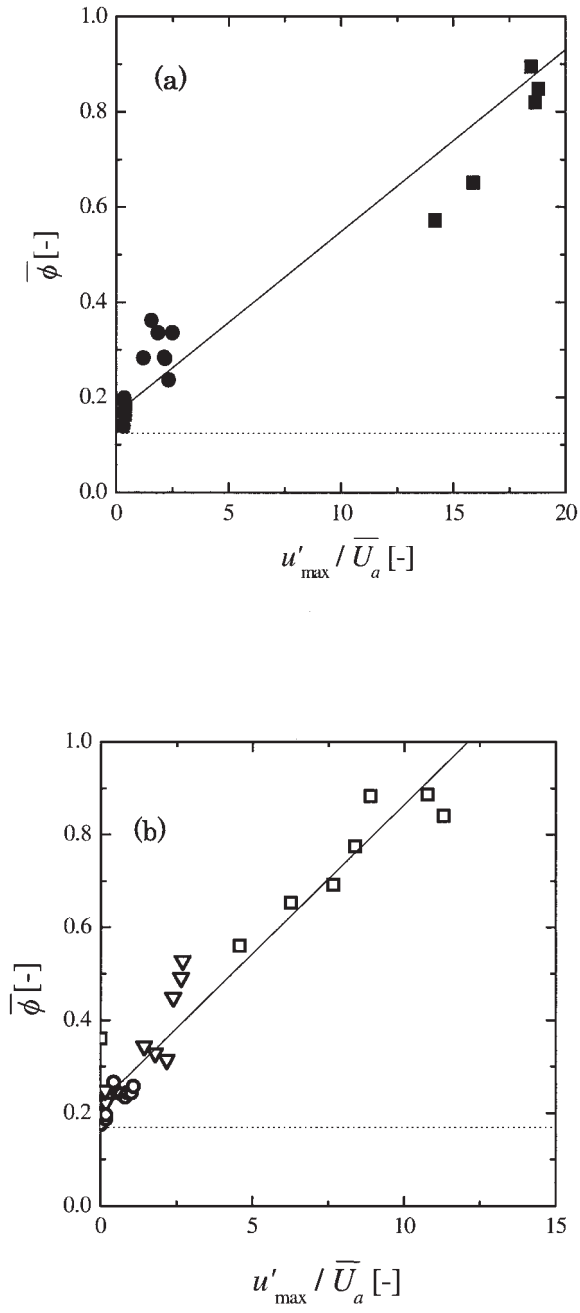

Figure 12. Relationship between the mixing rate and the normalized maximum rms value of streamwise fluid velocity fluctuation in (a) Runs I and II and (b) Runs III-IV.

(■) Run I; (●) Run II. (□) Run III; (▽) Run IV; (○) Run V.

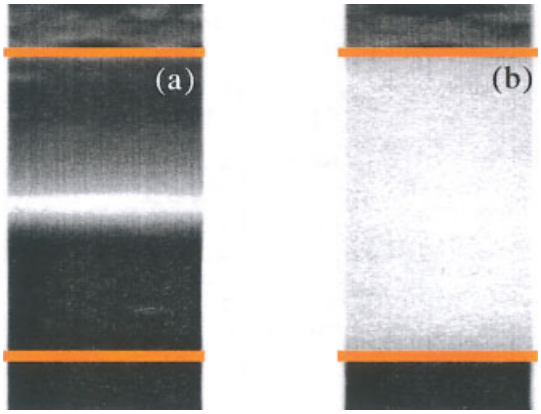

Figure 13. Images of the chemical product in Run I.

(a) No vibration ($u'_{max} = 0$); (b) Strong vibration with f_b = 92Hz (($u'_{max}/\bar{U}_a$ = 20.6). [Color figure can be viewed in the online issue, which is available at www.interscience.wiley.com.]

the configuration that the vibration system was set on the introductory tubes at 1m upstream to the microchannel. In other words, the proposed vibration system can be set far upstream from the microchannel, since the pressure fluctuation propagates in the long distance in a tube. We hope the proposed vibration technique can contribute to the development of a high-performance micro mixer and reactor.

Acknowledgments

The authors express great appreciation to Mrs. Naofumi Takenaka, Akihito Ito, and Kousuke Ishida for their assistance with the experiments. This research was supported by the New Energy and Industrial Technology Development Organization (NEDO).

Notation

A_t = vibration amplitude of the tube (beam) (mm)
C = normalized concentration (-)
Q = flow rate (ml/min)
Re = Reynolds number ($=lU_a/\nu$) (-)
S_v = power spectrum of the vertical velocity fluctuation of the tube (beam)
U, V, W = instantaneous velocity in the streamwise (x), vertical (y), and spanwise (z) directions (m/s)
f = vibration frequency (Hz)
f_b = basic vibration frequency (Hz)
l = channel width (mm)
u, v, w = velocity fluctuation in the streamwise, vertical, and spanwise directions (m/s)
V_{in} = electrical input for a vibrating motor (V)
x, y, z = coordinates in the streamwise, vertical, and spanwise directions (mm)

Greek letters

λ = wavelength of the Nd:YAG laser (nm)
ν = fluid dynamic viscosity (kg/m·s)
ϕ = cross-sectional mixing rate (-)
ξ = local mixing rate (-)

Subscripts

A = species A
B = species B
a = cross-sectionally averaged
max = maximum value at the cross section
t = tube (beam)
v = velocity

Superscripts

$\bar{}$ = time averaged
$'$ = rms value

Literature Cited

1. Ho CH, Tai YC. Micro-electro-mechanical-systems (MEMS) and fluid flows. *Annu Rev Fluid Mech.* 1998;30:579-612.
2. Stone HA, Stroock AD, Ajdari A. Engineering flows in small devices: microfluidics toward a lab-on-a-chip. *Annu Rev Fluid Mech.* 2004;36:381-411.
3. Ito Y, Nagata K, Komori S. The effects of high-frequency ultrasound on turbulent liquid mixing with a rapid chemical reaction. *Phys Fluids.* 2002;14:4362-4371.
4. Nagata K, Komori S. The effects of unstable stratification and mean shear on the chemical reaction in grid turbulence. *J Fluid Mech.* 2000;408:39-52.
5. Lee WY, Wong M, Zohar Y. Microchannels in series connected via a contraction/expansion section. *J Fluid Mech.* 2002;459:187-206.
6. Commenge JM, Falk L, Corriou JP, Matlosz M. Optimal design for flow uniformity in microchannel reactors. *AIChE J*. 2002;48:345-358.
7. Johnson TJ, Ross D, Locascio LE. Rapid microfluidic mixing. *Anal Chem*. 2002;74:45-51.
8. Ehrfeld W, Golbig K, Hessel V, Löwe H, Richter T. Characterization of mixing in micromixers by a test reaction: single mixing units and mixer arrays. *Ind Eng Chem Res*. 1999;38:1075-1082.
9. Beebe DJ, Adrian RJ, Olsen MG, Stremler MA, Aref H, Jo BH, Passive mixing in microchannels: fabrication and flow experiments. *Mec Ind*. 2001;2:343-348.
10. Jensen KF. Microreaction engineering—is small better? *Chem Eng Sci*. 2001;56:293-303.
11. Stroock AD, Dertinger SKW, Ajdari A, Igor M, Stone HA, Whitesides GM. Chaotic mixer for microchannels. *Science.* 2002;295:647-651.
12. Glasgow I, Aubry N. Enhancement of microfluidic mixing using time pulsing. *Lab on a Chip*. 2003;3:114-120.
13. Yang Z, Matsumoto S, Goto H, Matsumoto M, Maeda R. Ultrasonic micromixer for micro fluidic systems. *Sensors and Actuators A*. 2001;93:266-272.
14. Lin H, Storey BD, Oddy MH, Chen CH, Santiago JG. Instability of electrokinetic microchannel flows with conductivity gradients. *Phys Fluids*. 2004;16:1922-1935.
15. Sadr R, Yoda M, Zheng Z, Conlisk AT. An experimental study of electro-smotic flow in rectangular microchannel. *J Fluid Mech.* 2004;506:357-367.
16. Yi M, Qian S, Bau HH. A magnetohydrodynamic chaotic stirrer. *J Fluid Mech.* 2002;468:153-177.
17. Komori S, Ito Y. *Fluid Mixing Reaction Enhancement Method Using Micro Device, and Micro Device*. EP Patent No. CN1597077; 2005; and US Patent No. US2005058014(A1); 2005.

Manuscript received Oct. 10, 2005, and revision received May 11, 2006.